

## RESEARCH ARTICLE

# 11 $\beta$ -HSD1 inhibition does not affect murine tumour angiogenesis but may exert a selective effect on tumour growth by modulating inflammation and fibrosis

Callam T. Davidson<sup>1</sup>, Eileen Miller<sup>1</sup>, Morwenna Muir<sup>1,2</sup>, John C. Dawson<sup>2</sup>, Martin Lee<sup>2</sup>, Stuart Aitken<sup>1,3</sup>, Alan Serrels<sup>2</sup>, Scott P. Webster<sup>1</sup>, Natalie Z. M. Homer<sup>1,4</sup>, Ruth Andrew<sup>1</sup>, Valerie G. Brunton<sup>2,†</sup>, Patrick W. F. Hadoke<sup>1,4\*</sup>, Brian R. Walker<sup>1,5,†</sup>



**1** BHF Centre for Cardiovascular Science, The Queen's Medical Research Institute, University of Edinburgh, Edinburgh, United Kingdom, **2** Cancer Research UK Edinburgh Centre, Institute of Genetics & Molecular Medicine, University of Edinburgh, Edinburgh, United Kingdom, **3** MRC Human Genetics Unit, Institute of Genetics and Cancer, University of Edinburgh, Edinburgh, United Kingdom, **4** Edinburgh Mass Spectrometry Core, Clinical Research Facility, University of Edinburgh, Edinburgh, United Kingdom, **5** Institute of Genetic Medicine, Newcastle University, Newcastle University, Newcastle upon Tyne, United Kingdom

† These authors are joint senior authors on this work

\* [patrick.hadoke@ed.ac.uk](mailto:patrick.hadoke@ed.ac.uk)

## OPEN ACCESS

**Citation:** Davidson CT, Miller E, Muir M, Dawson JC, Lee M, Aitken S, et al. (2023) 11 $\beta$ -HSD1 inhibition does not affect murine tumour angiogenesis but may exert a selective effect on tumour growth by modulating inflammation and fibrosis. PLoS ONE 18(3): e0255709. <https://doi.org/10.1371/journal.pone.0255709>

**Editor:** Sripathi M Sureban, University of Oklahoma Health Sciences Center, UNITED STATES

**Received:** July 20, 2021

**Accepted:** December 5, 2022

**Published:** March 20, 2023

**Copyright:** © 2023 Davidson et al. This is an open access article distributed under the terms of the [Creative Commons Attribution License](#), which permits unrestricted use, distribution, and reproduction in any medium, provided the original author and source are credited.

**Data Availability Statement:** All relevant data are within the paper.

**Funding:** CT Davidson was funded by a British Heart Foundation studentship (Award Number: FS/13/52/30637). EM was supported by a British Heart Foundation Project Grant (Award Number PG/15/10/31277; PWFH; BRW). MM and ML were funded by the Cancer Research UK Edinburgh Centre (C157/A25140). The study was supported by the British Heart Foundation (Award Number:

## Abstract

Glucocorticoids inhibit angiogenesis by activating the glucocorticoid receptor. Inhibition of the glucocorticoid-activating enzyme 11 $\beta$ -hydroxysteroid dehydrogenase type 1 (11 $\beta$ -HSD1) reduces tissue-specific glucocorticoid action and promotes angiogenesis in murine models of myocardial infarction. Angiogenesis is important in the growth of some solid tumours. This study used murine models of squamous cell carcinoma (SCC) and pancreatic ductal adenocarcinoma (PDAC) to test the hypothesis that 11 $\beta$ -HSD1 inhibition promotes angiogenesis and subsequent tumour growth. SCC or PDAC cells were injected into female FVB/N or C57BL6/J mice fed either standard diet, or diet containing the 11 $\beta$ -HSD1 inhibitor UE2316. SCC tumours grew more rapidly in UE2316-treated mice, reaching a larger (P<0.01) final volume ( $0.158 \pm 0.037 \text{ cm}^3$ ) than in control mice ( $0.051 \pm 0.007 \text{ cm}^3$ ). However, PDAC tumour growth was unaffected. Immunofluorescent analysis of SCC tumours did not show differences in vessel density (CD31/alpha-smooth muscle actin) or cell proliferation (Ki67) after 11 $\beta$ -HSD1 inhibition, and immunohistochemistry of SCC tumours did not show changes in inflammatory cell (CD3- or F4/80-positive) infiltration. In culture, the growth/viability (assessed by live cell imaging) of SCC cells was not affected by UE2316 or corticosterone. Second Harmonic Generation microscopy showed that UE2316 reduced Type I collagen (P<0.001), whilst RNA-sequencing revealed that multiple factors involved in the innate immune/inflammatory response were reduced in UE2316-treated SCC tumours. 11 $\beta$ -HSD1 inhibition increases SCC tumour growth, likely via suppression of inflammatory/immune cell signalling and extracellular matrix deposition, but does not promote tumour angiogenesis or growth of all solid tumours.

RG/11/4/28734 (BRW, RA); [www.bhf.org.uk](http://www.bhf.org.uk))

Cancer Research UK (Award Number: C157/

A24837 (VGB) and the Wellcome Trust (Award Number: 107049/Z/15/Z (BRW); [wellcome.org](http://wellcome.org)). The funders had no role in study design, data collection and analysis, decision to publish, or preparation of the manuscript.

**Competing interests:** Brian Walker, Patrick Hadoke and Scott Webster are inventors on relevant patents owned by the University of Edinburgh (see below). Additionally, Brian Walker reports consultancy fees as part of membership of Actinogen Medical's Scientific Advisory Board, related to 11 $\beta$ -hydroxysteroid dehydrogenase type I inhibitors, and Scott Webster and Ruth Andrew report consultancy fees from Actinogen Medical unrelated to the current work. Callam Davidson is an editor for PLOS Medicine. This does not alter our adherence to PLOS ONE policies on sharing data and materials.

## Introduction

Glucocorticoids are vital modulators of the physiological stress response, exerting myriad effects across a range of tissues [1]. Their potent anti-inflammatory and immunosuppressive effects have also been exploited clinically for more than half a century; synthetic glucocorticoids are commonly used to treat chronic inflammatory conditions such as rheumatoid arthritis, to suppress the immune system before organ transplant, and in the treatment of leukemia [2].

The adverse consequences of chronic glucocorticoid excess are exemplified in people with Cushing's syndrome, who develop increased central adiposity, dyslipidemia, muscle wasting, loss of memory, hyperglycaemia and insulin resistance [1]. Reducing glucocorticoid action in key target tissues, such as liver, adipose and brain, may therefore be clinically desirable, but targeting the hypothalamic-pituitary-adrenal (HPA) axis risks compromising the systemic coordination of the stress response.

Glucocorticoids are subject to tissue-specific pre-receptor regulation by the 11 $\beta$ -hydroxysteroid (11 $\beta$ -HSD) isozymes; 11 $\beta$ -HSD2 converts cortisol or corticosterone to inert 11-keto metabolites (cortisone or 11-dehydrocorticosterone, respectively) to allow selective access of aldosterone to mineralocorticoid receptors (MR), while 11 $\beta$ -HSD1 re-activates glucocorticoids by catalyzing the reverse reductase reaction in target tissues [3], including liver, adipose, brain and the blood vessel wall [4]. Preclinical investigations have demonstrated that 11 $\beta$ -HSD2 inhibition can reduce myocardial fibrosis in a rat (uni-nephrectomy) model [5] whilst inhibition of 11 $\beta$ -HSD1 reduced hepatic steatosis in mice fed a high fat diet [6]. Targeting 11 $\beta$ -HSD1 offers a novel therapeutic avenue to reduce glucocorticoid action. Clinical trials of 11 $\beta$ -HSD1 inhibitors have shown moderate improvements in glycaemic control in patients with type II diabetes [7], and more recently have shown promise in the treatment of cognitive decline [8].

Glucocorticoids also exert potent angiostatic effects, an activity first shown over 30 years ago but the mechanism of which remains uncertain [9]. Inhibition or deletion of 11 $\beta$ -HSD1 promotes angiogenesis *in vitro* and *in vivo*, enhancing wound healing, reducing intra-adipose hypoxia and, most strikingly, enhancing recovery after myocardial infarction in mice [10–14]. Whilst presenting a potential clinical opportunity, these findings have also raised concerns that 11 $\beta$ -HSD1 inhibitors could exacerbate conditions characterised by pathological angiogenesis, such as proliferative diabetic retinopathy and solid tumour growth [15]. Whereas 11 $\beta$ -HSD1 inhibition or deletion was recently shown not to promote angiogenesis in a model of proliferative retinopathy [16], there is evidence to suggest it could influence tumour growth [17]. Moreover, not only might 11 $\beta$ -HSD1 inhibitors act in vascular cells to promote tumour angiogenesis, but they might also directly influence tumour cells as well as other cells in the tumour microenvironment, including fibroblasts, and tumour-associated immune cells [18].

The only study to address this topic thus far demonstrated that overexpression of 11 $\beta$ -HSD1 in hepatocellular carcinoma cells reduced tumour growth and angiogenesis [17]. No study has yet examined the effects of 11 $\beta$ -HSD1 inhibition on tumour growth. Of note, expression of 11 $\beta$ -HSD1 and the glucocorticoid receptor (GR) are particularly high in squamous cell carcinoma (SCC) [19], highlighting this tumour type as potentially glucocorticoid-sensitive. The present study tested the hypothesis that 11 $\beta$ -HSD1 inhibition promotes the growth of subcutaneously-implanted SCC and pancreatic ductal adenocarcinoma (PDAC) tumours in mice, as a result of increased tumour angiogenesis.

## Material and methods

### Animals

In total, 18 C57BL6/J and 18 FVB/N mice were purchased from Envigo (Blackthorn, UK) or Charles River (Elphinstone, UK), respectively. All experimental animals were female and aged 9–14 weeks and sacrificed by cervical dislocation. Groups were age-matched. All procedures were approved by the institutional ethical committee and carried out by a licensed individual and in strict accordance with the Animals (Scientific Procedures) Act 1986 and the EU Directive 2010/63 and under project licence 70/8897 or 60/4523.

### Cell culture

Studies made use of two immortalised murine cancer cell lines. SCC cells [20] were generated in-house by Dr Alan Serrels using a two-stage 7,12-Dimethylbenz[a]anthracene (DMBA)/TPA chemical carcinogenesis protocol [21]. A PDAC cell line, Panc043, was provided by the Beatson Institute in Glasgow; these cells were originally derived from tumours developed using the *LSL-KrasG12D/+; LSL-Trp53R172H/+; Pdx-1-Cre* (KPC) model [22]. Panc-043 cells were cultured in Dulbecco's Modified Eagle Medium (DMEM) supplemented with 10% FCS. SCC cells were maintained in Glasgow Minimum Essential Medium (GMEM) supplemented with 10% FCS, 2mM L-Glutamine, 1mM sodium pyruvate, MEM non-essential amino acids (Thermo-Fisher) and MEM vitamins.

Tumour cells (SCC or Panc043) were cultured in 96-well plates (Bio-Greiner; 5000 cells per well) and treated with 25–300nM UE2316 or corticosterone. Plates were imaged and confluence determined using the Incucyte ZOOM Live-cell analysis system (over 72 hours; Essen BioScience). An alamarBlue assay (Thermo-Fisher) was also performed as per manufacturer's instructions to provide a secondary measure of viable cell number.

### Drugs and corticosteroids

The 11 $\beta$ -HSD1 inhibitor UE2316 ([4-(2-chlorophenyl-4-fluoro-1-piperidinyl][5-(1H-pyrazol-4-yl)-3-thienyl]-methanone) was synthesised by High Force Ltd (Durham, UK) [23]. For *in vivo* studies, UE2316 was delivered *ad libitum* to animals added to a RM1 diet (175mg/kg UE2316) prepared by Special Diet Services (Essex, UK). 11-Dehydrocorticosterone and corticosterone were from Steraloids (Newport, USA). Tritiated steroids ([1,2,6,7]- $^3$ H<sub>4</sub>-corticosterone and [1,2,6,7]- $^3$ H<sub>4</sub>-cortisone) were from PerkinElmer (Wokingham, UK).

### Tumour model

*In vivo* studies used an established model of subcutaneous tumour development [24]. SCC or PDAC cells were injected subcutaneously (1x10<sup>6</sup> cells/flank) into FVB/N or C57BL6/J mice, respectively, fed either control or UE2316 diet for 5 days in advance of injection and throughout the remainder of the experiment (N = 6–9/group). Diet was weighed regularly to monitor consumption, which did not differ between diets. SCC tumours were grown for 11 days, PDAC tumours were grown for 14 days, and both were measured using calipers every 2–3 days. Tumour volume was calculated as the volume of an ellipsoid (0.5\*length\*breadth<sup>2</sup>).

Animals were weighed and checked for signs of unexpected ill health every 2–3 days. Weight loss of >20% between measurements was considered grounds for humane termination, as were any tumour-related limitations in the animal's normal behavioural repertoire (e.g., impeded movement) or a body conditioning score of 2 being reached. Animals were to be culled prior to the pre-defined experimental endpoint if tumours reached maximum

permissible size (15 mm diameter), or if signs of ulceration were evident. Mice were culled by cervical dislocation.

### Histology

**Vessel staining.** Paraffin-embedded tumour sections underwent rehydration and heat-based antigen retrieval. Sections were permeabilised (0.4% Triton-X, 15 min) and blocked (1% normal goat serum, 30 min; Biosera, Nuaille, France), incubated with primary CD31 antibody (1/300 dilution, 18h, 4°C, Ab28364; Abcam, Cambridge, UK), rinsed with PBS and incubated with secondary antibody and primary conjugated  $\alpha$ -smooth muscle actin antibody (1/1000 dilution, 1 hour, room temperature, A-11034; Molecular Probes, Eugene, USA. C6198; Sigma) before counterstaining with DAPI (5 min) and mounting using Fluoromount G (SouthernBiotech, Cambridge, UK). Slides were imaged with an Axioscan.Z1 (Zeiss) digital slide scanner. Higher magnification images were obtained using a LSM710 confocal microscope (Zeiss). Vessels were manually counted by a blinded observer across 10 randomly selected 0.1mm<sup>2</sup> fields of view, from two tumour sections spaced 50  $\mu$ m apart. CD31-positive/ $\alpha$ -SMA-negative vessels and CD31/ $\alpha$ -SMA-positive vessels were both quantified to allow the ratio of vessels with smooth muscle coverage to be calculated. As a secondary measure of vessel density, sections stained for CD31 were quantified by Chalkley count, as described [25]. One section (three hot-spots) was quantified per tumour.

**In vivo tumour cell proliferation.** Tumour sections were stained with Ki67 antibody (proliferation marker, 1/100 dilution, Ab155580; Abcam) as above. 2 sections/tumour were scanned at 200x magnification, the most proliferative region selected by eye, and this region then imaged at 400x magnification. Ki67-positive cells were then quantified manually per hotspot.

**Immune/Inflammatory cell staining.** F4/80 (1/300, 14-4801; eBiosciences) and CD3 (1/100, Sc-20047; Santa-Cruz) staining were performed using the Leica BOND-III automated staining system and the Leica refine detection kit as per manufacturer's instructions (Leica). Trypsin-based antigen retrieval was used for F4/80 staining, and heat-based antigen retrieval for CD3 staining. Dehydrated sections were mounted with DPX and imaged using the slide scanner. Images were segmented and stain percentage area was quantified automatically using ImageJ software.

### Enzyme activity assays

A BioRad protein DC assay (BioRad, Hemel-Hempsted, UK) was performed as per manufacturer's instructions.

**Dehydrogenase activity assay.** Homogenized tumour samples were diluted in assay buffer (63g glycerol, 8.77g NaCl, 186mg ethylenediaminetetraacetic acid (EDTA), 3.03g Tris, made up to 500mL with distilled H<sub>2</sub>O and pH adjusted to 7.7). <sup>3</sup>H<sub>4</sub>-Corticosterone (250nM) and NADP<sup>+</sup> (2mM; Cambridge Bioscience) were added before incubation in a shaking water bath (37°C). After incubation, samples were extracted with ethyl acetate (10:1), dried under nitrogen and dissolved in 65:15:25 water/acetonitrile/methanol.

**Reductase activity assay.** C57BL6/J mouse liver was excised and sectioned. Liver pieces (5-20mg, N = 6/group) were cultured in 1mL DMEM-F12 medium containing 12.5nM <sup>3</sup>H<sub>4</sub>-cortisone and 1 $\mu$ M cold cortisone with either 300nM UE2316 or vehicle (final DMSO concentration 0.3%). Plates were incubated for 24 hours (5% CO<sub>2</sub>, 37°C). Media was extracted on Sep-Pak C-18 (360mg) cartridges (Waters, Elstree, UK), dried under nitrogen, resuspended in 200 $\mu$ L HPLC-grade H<sub>2</sub>O added, and extracted with ethyl acetate (10:1) to remove phenol red contamination, dried under nitrogen and dissolved in 60:40 water/methanol.

### Second harmonic generation imaging

Type I collagen was visualized in SCC and PDAC tumours (N = 6/group) by Second Harmonic Generation (SHG) microscopy. A pump laser (tuned to 816.8 nm, 7 ps, 80 MHz repetition rate; 50 mW power at the objective) and a spatially overlapped second beam, termed the Stokes laser (1064 nm, 5–6 ps, 80 MHz repetition rate, 30 mW power at the objective; picoEmerald (APE) laser) was inserted into an Olympus FV1000 microscope coupled with an Olympus XLPL25XWMP N.A. 1.05 objective lens with a short-pass 690 nm dichroic mirror (Olympus). The Second Harmonic Generation signal was filtered (FF552-Di02, FF483/639-Di01 and FF420/40) and images quantified using Image J.

### qPCR

Frozen tissue was homogenized in Qiazol reagent (Qiagen), allowed to settle at room temperature for 5 min, vortexed in chloroform and left to settle for 2 min before centrifugation (12000 RCF x 15 min at 4°C). The resultant aqueous phase was mixed with an equal volume of 70% ethanol. All subsequent on-column steps were performed as per the RNeasy manufacturer's protocol. RNA concentration and integrity were assessed using the Nano-drop 1000 (Thermo-Fisher Scientific). cDNA was generated from RNA using the Quanti-Tect Reverse Transcription Kit (Qiagen) as per manufacturer's protocol. For the PCR reaction, samples were incubated at 42° for 15 min followed by 95° for 3 min in a Thermal cycler (Techne-Cole-Palmer, Staffordshire, UK). cDNA was diluted 1/40 in RNase-free water and a standard curve constructed by serial dilution of a pooled sample. In triplicate on a 384-well plate, 2 $\mu$ L of sample were combined with 5 $\mu$ L of Lightcyler 480 Probes Master mastermix (Roche), primers (0.1 $\mu$ L/sample Forward and Reverse), probe (0.1 $\mu$ L/sample) and RNase-free water to make up to 10 $\mu$ L total volume. Plates were spun (420 RCF x 2 min on LCM-3000 plate centrifuge (Grant Instruments, Royston, UK) before analysis on the Light Cycler 480 (Roche). Samples were run for 50 cycles (10s at 95°C and 30s at 60°C). All data were normalised to the average of two housekeeping genes (*Gapdh* and *Tbp*).

### RNA sequencing

RNA from SCC tumours, extracted as described above, was sequenced by GATC Biotech (Constance, Germany). Raw data were processed using Tophat2 [26], which was used to map reads to the mouse mm10 reference genome. Differential gene expression was analysed using Cuffdiff [27]. DEseq2 was used to perform a Principle Component Analysis (PCA) to assess variance between samples. Gene ontology analysis was performed using the Database for Annotation, Visualization and Integrated Discovery (DAVID) v6.8.

### Data analysis and statistics

All statistics were performed using Prism software v6/7 (Graphpad). Data are presented as mean  $\pm$  S.E. Outliers were identified using Grubbs' test and excluded appropriately. All data sets were tested for a parametric distribution and transformed/analysed appropriately. N refers to the number of animals per group in an experiment, with the exception of cell culture studies in which N refers to biological repeats on separate days using the same cell line. P<0.05 was considered significant.

## Results

### 11 $\beta$ -HSD1 is expressed in SCC but not PDAC tumour cell lines

When comparing 11 $\beta$ -HSD1 dehydrogenase activity between tumour types, SCC tumours showed a considerably higher rate of product formation than PDAC (Fig 1A) and showed higher GR expression (Fig 1B). 11 $\beta$ -HSD2 was not detected in either tumour type.

### 11 $\beta$ -HSD1 inhibition enhances SCC tumour growth

UE2316 accelerated the growth of SCC tumours from day 4 onwards (Fig 2A) but had no effect on the growth of PDAC tumours (Fig 2B). UE2316 and control diet fed groups consumed similar quantities of diet and did not differ in weight throughout the experiment (Fig 2C). The estimated dosage achieved in the present studies (based on diet consumed per cage per 2–3 days) was 25–30mg/kg/mouse/day. Ki67 staining revealed a trend towards reduced tumour cell proliferation in UE2316-treated SCC tumours compared to control tumours, but this did not reach significance (Fig 2D–2F).

### 11 $\beta$ -HSD1 inhibition does not promote angiogenesis in SCC tumours

The effect of 11 $\beta$ -HSD1 inhibition on vessels in tumours was assessed by CD31/ $\alpha$ -SMA-positive staining (Fig 3A and 3B). In SCC and PDAC tumours, UE2316 did not affect the number of blood vessels per field of view (Fig 3C) or the vessel number determined by Chalkley counts (Fig 3E). In SCC tumours, UE2316 did not affect the proportion of immature vessels lacking smooth muscle coverage, assessed by CD31 staining in the absence of  $\alpha$ -SMA staining (Fig 3D). UE2316 also did not affect mRNA levels for angiogenic factors *Vegfa* and *Vegfr2* in either tumour type (Fig 3F).

### Neither corticosterone nor UE2316 affect SCC cell proliferation *in vitro*

SCC cells in culture were imaged using the Incucyte ZOOM live cell imaging system to investigate the effects of glucocorticoids and UE2316 on cell growth and morphology. Addition of increasing concentrations of corticosterone (Fig 4A) or UE2316 (Fig 4B) had no effect on the growth of SCC cells over 72 hours. Neither corticosterone (Fig 4C) nor UE2316 (Fig 4D) affected cell viability at any concentration, assessed after 72 hours using an alamarBlue assay.

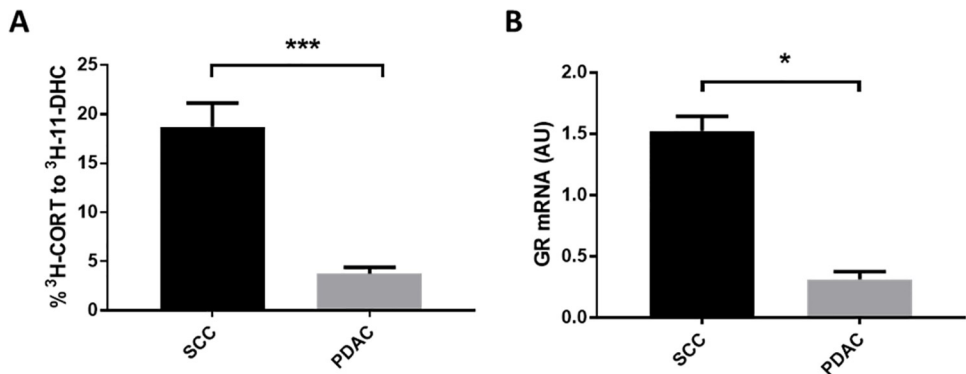


**Fig 1. SCC tumours show greater 11 $\beta$ -HSD1 activity and express more GR than PDAC tumours.** A) SCC tumours had greater 11 $\beta$ -HSD1 dehydrogenase activity than PDAC tumours. \*\*\*  $P < 0.001$ . N = 6/group. B) GR transcript levels were greater in SCC tumours than PDAC tumours. N = 5–6/group. \*  $P < 0.05$ . Data were compared by independent sample t-test.

<https://doi.org/10.1371/journal.pone.0255709.g001>

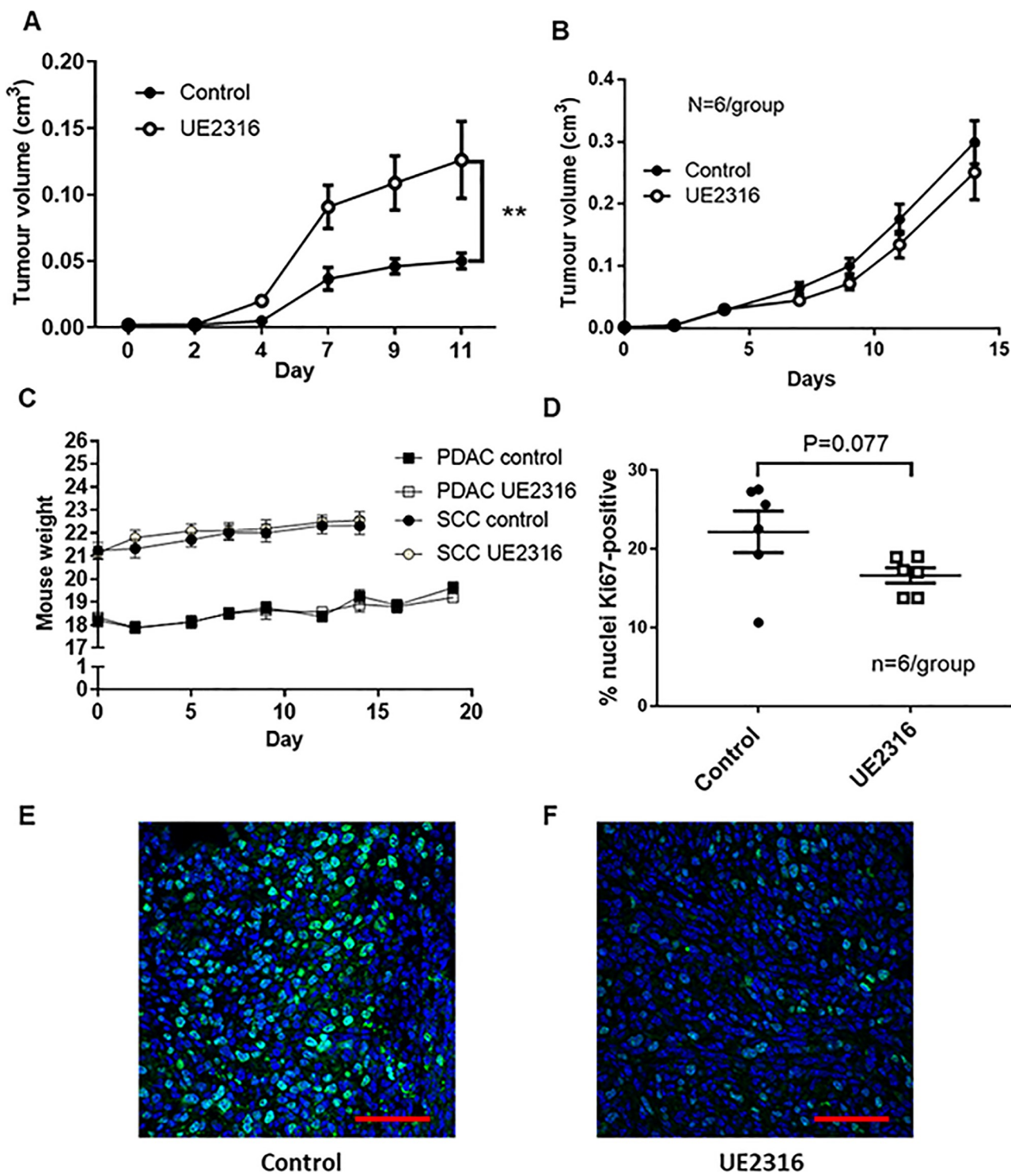


**Fig 2. The 11 $\beta$ -HSD1 inhibitor UE2316 enhances SCC but not PDAC tumour growth.** A) UE2316 enhanced tumour growth from day 4 onwards in mice injected with SCC cells. N = 9/group. B) UE2316 did not affect PDAC tumour growth in mice injected with Panc043 cells. N = 6/group. C) Neither tumour cell injection (day 5) nor UE2316 diet introduction affected mouse weight. N = 6-9/group. \*\* P < 0.01. Data were compared by 2-Way ANOVA. D) The proportion of cells staining positive for proliferation marker Ki67 showed a trend towards being reduced (P = 0.07) in tumours from UE2316-treated mice but this did not reach significance. N = 6/group. Data were compared by independent samples t-test. Representative images of hotspots from Ki67-stained squamous cell carcinoma (SCC) tumours from control (E) and UE2316 treated (F) mice are shown. Hotspots were typically near the periphery of the tumour. Scale bar = 50 $\mu$ m.

<https://doi.org/10.1371/journal.pone.0255709.g002>

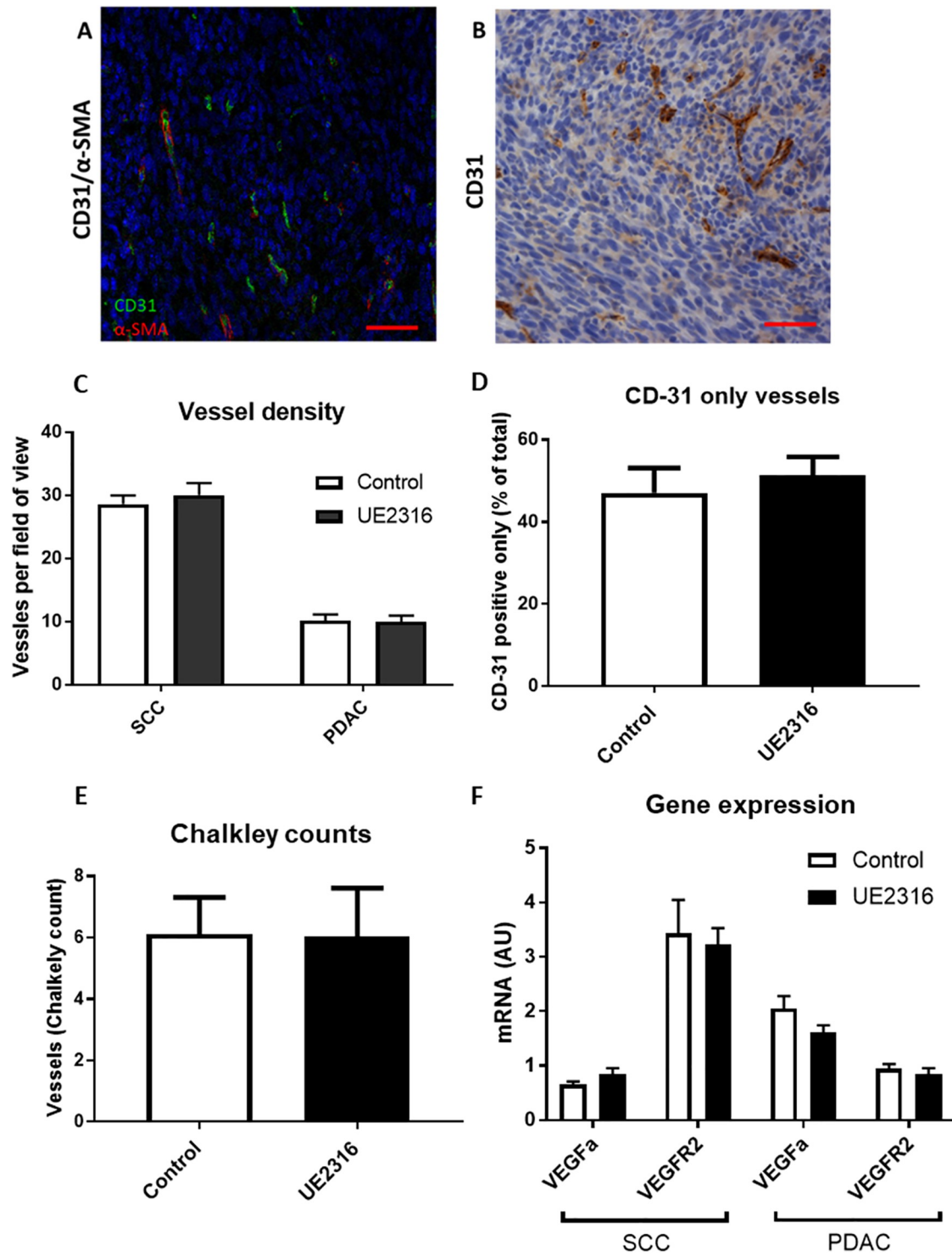


**Fig 3. UE2316 does not affect angiogenesis in tumours.** A) Tumour tissue from SCC tumours; endothelial cells are stained green (CD31 visualised with Alexa-Fluor 488), smooth muscle cells are stained red ( $\alpha$ -SMA visualised with Cy3) and nuclei are stained blue (DAPI). Tumours had densely packed nuclei. 200x magnification. Scale bar 50 $\mu$ m. B) CD31 was also visualised with diaminobenzidine (DAB) for counts. 200x magnification. Scale bar 50 $\mu$ m. C) UE2316 did not affect vessel density in either SCC or PDAC tumours. D) UE2316 did not affect the proportion of vessels lacking smooth muscle coverage in SCC tumours (i.e. CD31 positive but  $\alpha$ -SMA negative). (E) UE2316 did not affect Chalkley counts in SCC tumours. 1 section/tumour, N = 5–6 animals/group. F) mRNA levels for *Vegfa* and *Vegfr2* in SCC tumours were unaffected by UE2316. Data were compared by independent samples t-test for panels C/D, Mann-Whitney U test for Panel E.

<https://doi.org/10.1371/journal.pone.0255709.g003>

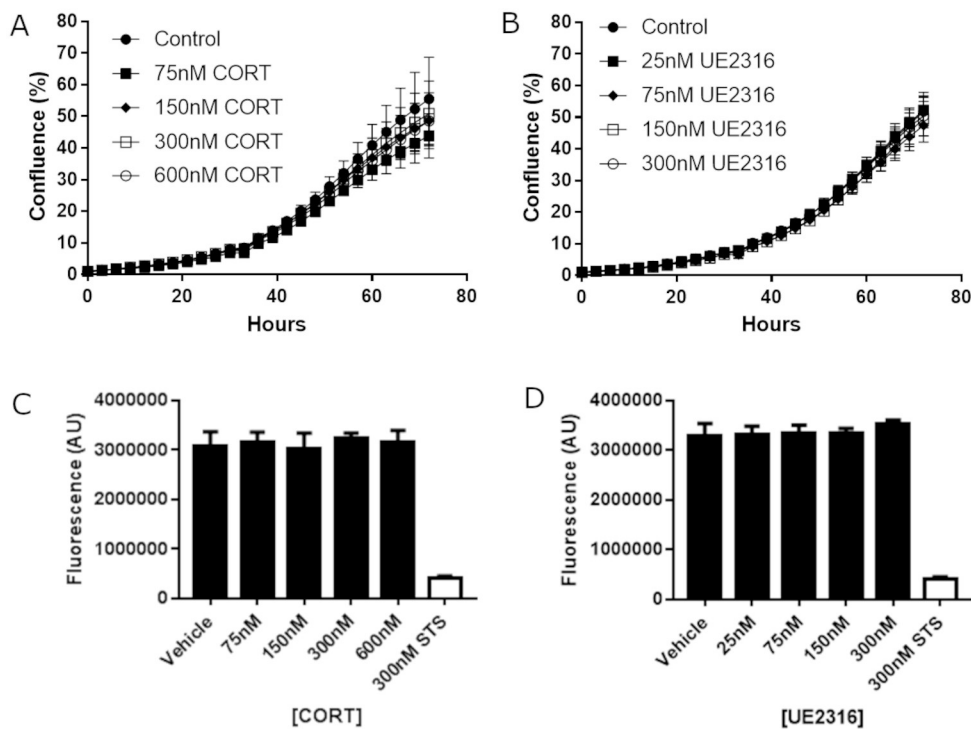


**Fig 4. Neither corticosterone nor UE2316 affect SCC cell growth or viability *in vitro*.** The confluence of SCC cells imaged over 72 hours using the Incucyte was unaffected by exposure to either corticosterone (CORT, panel A) or the 11 $\beta$ -HSD1 inhibitor UE2316 (panel B). 300nM STS was included in all experiments as a positive cytotoxic control. N = 5 (technical repeats, treatments in sextuplet). SCC viability, as determined by the alamarBlue assay, was unaffected by the addition of corticosterone (panel C) or the 11 $\beta$ -HSD1 inhibitor UE2316 (panel D). AU = Arbitrary units. N = 4 (technical repeats, treatments in sextuplet). Data were compared by one-way ANOVA.

<https://doi.org/10.1371/journal.pone.0255709.g004>

### 11 $\beta$ -HSD1 inhibition does not alter F4/80- or CD3- positive cell infiltration into SCC tumours

To quantify inflammatory cell content, sections from SCC tumours from control (Fig 5A) and UE2316-diet-fed mice (Fig 5B; N = 6/group) were labelled with F4/80 antibody, a macrophage marker. The antibody produced a cytoplasmic stain, present across the tumour but concentrated at the tumour periphery and in regions near the centre of the tumour. There was no significant difference in F4/80-positive area in tumours from RM-1 and UE2316 diet-fed mice, despite a trend towards a decrease in UE2316-treated tumours (Fig 5C). To quantify infiltrating T-cells, SCC tumours from control and UE2316-diet-fed mice (N = 5/group) were labelled with anti-CD3 to identify CD3-positive cells. There was no significant difference in CD3-positive area in tumours from RM-1 and UE2316 diet-fed mice (Fig 5D); representative images are shown in Fig 5E and 5F.

### 11 $\beta$ -HSD1 inhibition reduces type 1 collagen deposition in SCC tumours

To determine whether tumour collagen deposition was altered by 11 $\beta$ -HSD1 inhibition, Second Harmonic Generation (SHG) microscopy was performed on SCC tumours (N = 6/group; Fig 6A and 6B). Automatic quantification of % collagen area from SHG images revealed a reduced amount of type I collagen in tumours from mice fed UE2316-diet compared to tumours from mice fed normal diet (Fig 6C). This difference was also apparent at a transcriptional level (Fig 6D).

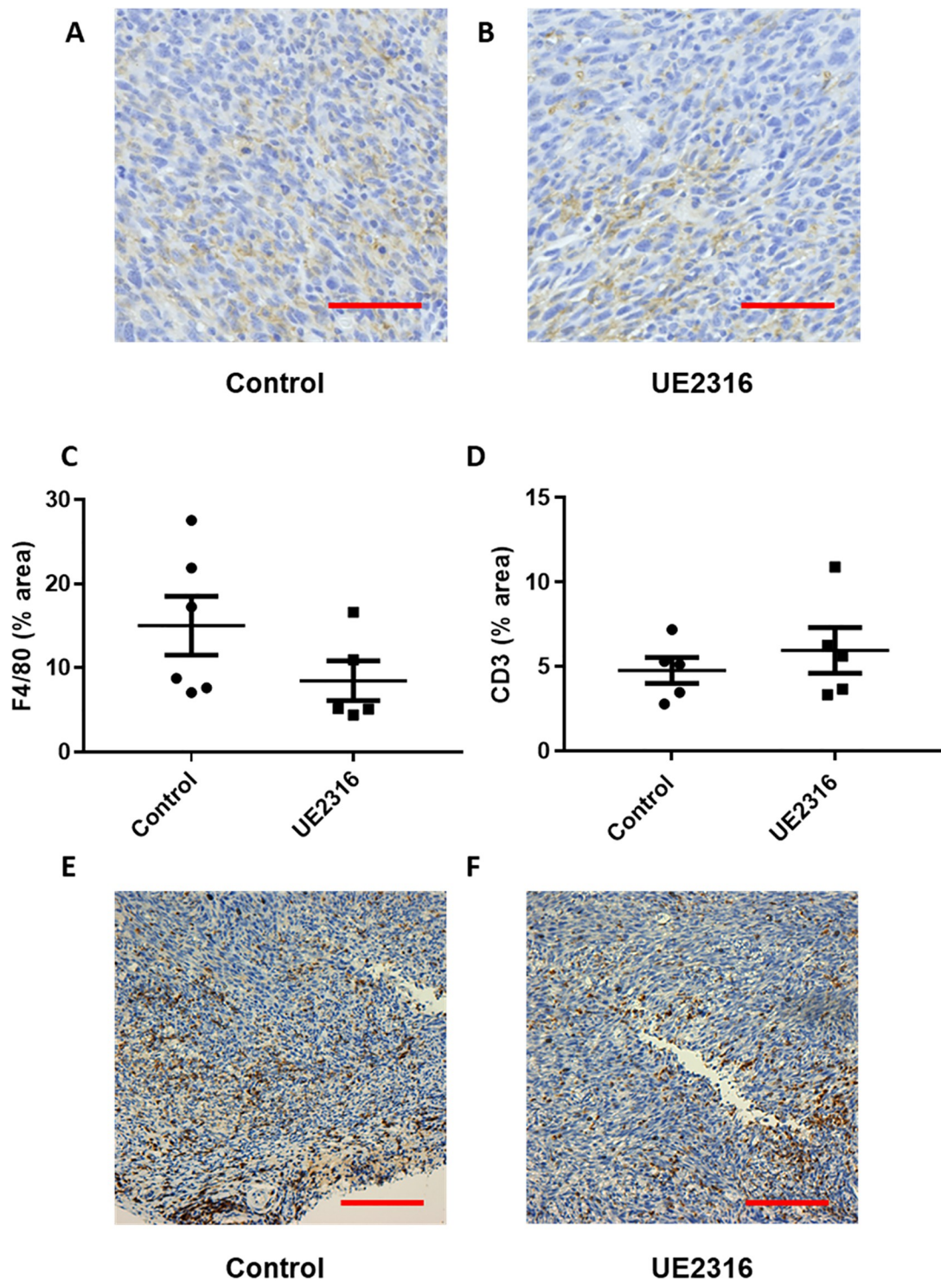


**Fig 5. F4/80 and CD3 positive cell number in SCC tumours were unaffected by UE2316.** Representative images of squamous cell carcinoma (SCC) tumours from control (A) and UE2316-treated (B) mice are shown, with DAB immunoreactivity to anti-F4/80 antibody shown in brown and haematoxylin-counterstained nuclei in blue. C) Immunostaining did not reveal a difference in F4/80-positive stain area between tumour from control and UE2316-treated mice ( $P = 0.17$ ). N = 5-6/group. Data were compared by independent samples t-test. Scale bar = 50 $\mu$ m. Immunostaining found no difference in CD3-positive stain area between SCC tumours from control and UE2316-treated mice, assessed by whole section analysis. N = 5/group (D). Representative images of CD3 labelled SCC tumour sections from control (E) and UE2316-treated (F) squamous cell carcinoma (SCC). DAB immunoreactivity shown in brown and haematoxylin-counterstained nuclei in blue. Data were compared by independent samples t-test, N = 5/group.

<https://doi.org/10.1371/journal.pone.0255709.g005>

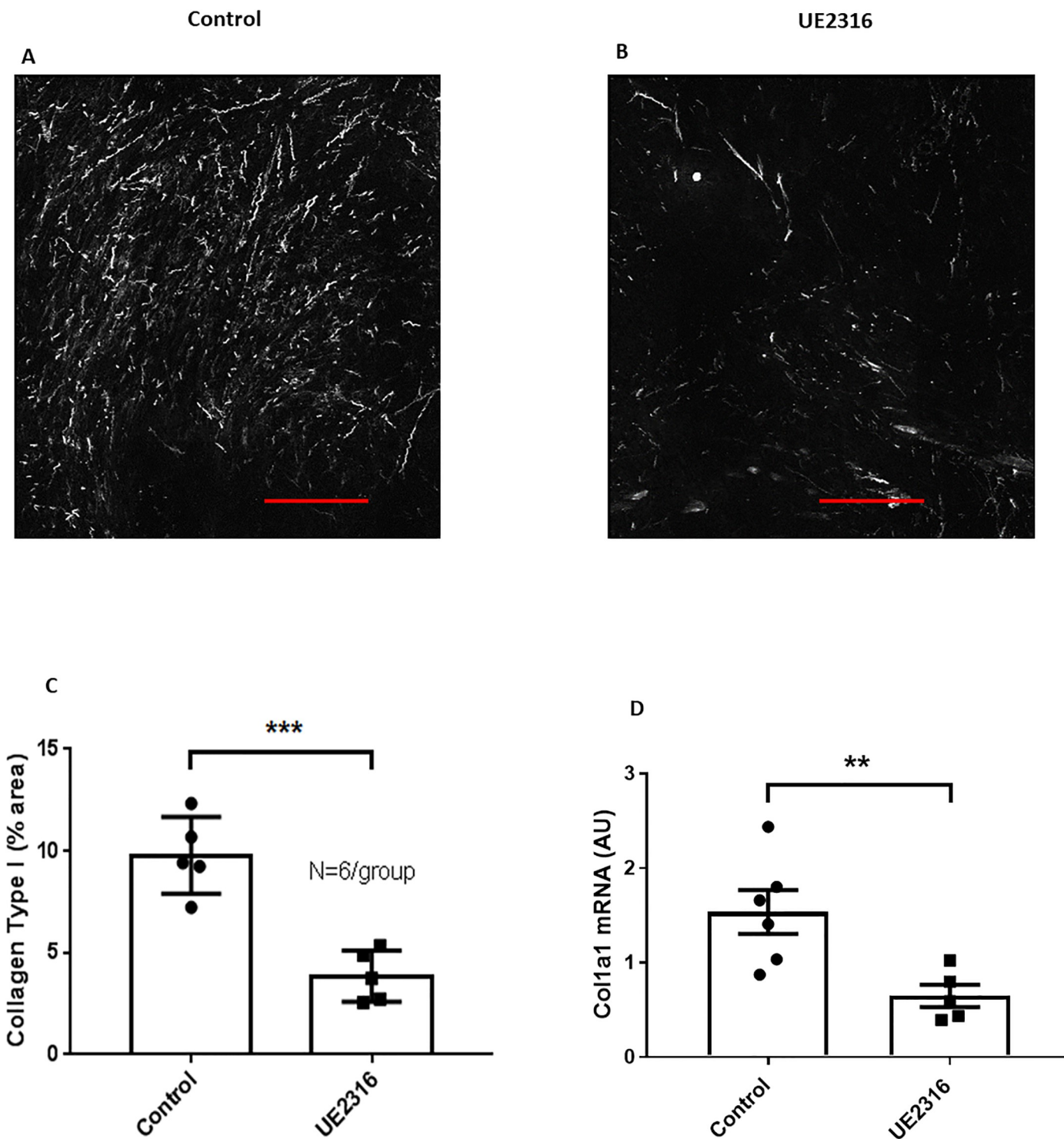


**Fig 6. Type I collagen is reduced in SCC tumours from UE2316-treated mice.** Second Harmonic Generation imaging showed type I collagen (white signal) in SCC tumours from UE2316-treated (B) and control mice (A). Scale bar = 100 $\mu$ m. C) Type I collagen was reduced in tumours from UE2316-treated mice. \*\*\* P<0.001. N = 5/group. D) *Col1a1* mRNA was reduced in SCC tumours from UE2316-treated mice compared to control mice. AU = Arbitrary units. \*\* P<0.01. N = 5-6/group. Data were compared by independent samples t-test.

<https://doi.org/10.1371/journal.pone.0255709.g006>

## 11 $\beta$ -HSD1 inhibition influences immune and inflammatory signaling in SCC tumours

Genes found to be differentially expressed (DE) between control and UE2316-treated SCC tumours by RNA sequencing were analysed using the Database for Annotation, Visualization and Integrated Discovery (DAVID) v6.8. 674 genes were found to be differentially regulated between treatment groups. Significantly relevant ( $P < 0.05$ ) biological processes are listed in [Table 1](#). Given the importance of local glucocorticoids in regulating inflammation, and the chronic inflammatory state of the tumour microenvironment, genes associated with the inflammatory response and immune response (6.1% and 4.1% of DE genes respectively, as identified by DAVID) and their relative expression in UE2316-treated tumours (as identified by RNA-seq) are shown in [Fig 7A and 7B](#). mRNA coding for a large number of pro-inflammatory cytokines were reduced after UE2316 treatment, while mRNA for cytokine receptors, toll-like receptor and mast cell protease transcript was increased.

## Discussion

The data generated in this investigation demonstrate that 11 $\beta$ -HSD1 inhibition can promote SCC tumour growth in mice. This effect was not seen in PDAC tumours, which expressed lower levels of both GR and 11 $\beta$ -HSD1 than SCC. The present findings are in agreement with

**Table 1.**

Process	q-value
Inflammatory response	3E-08
Cellular response to interferon-beta	4E-07
Positive regulation of gene expression	3E-04
Immune response	6E-04
Response to lipopolysaccharide	0.001
Positive regulation of cell migration	0.001
Chemokine-mediated signalling pathway	0.004
Cellular response to interferon- $\gamma$	0.004
Negative regulation of osteoblast differentiation	0.003
Chemotaxis	0.008
Collagen fibril organization	0.008
Defence response to virus	0.007
Positive regulation of apoptotic process	0.008
Circadian rhythm	0.009
Osteoblast differentiation	0.01
Negative regulation of cell migration	0.03
Cell adhesion	0.04
Ossification	0.04
Immune system process	0.05
Positive regulation of osteoblast differentiation	0.05
Defense response to protozoan	0.05

Gene ontology analysis of RNA-seq data demonstrates the importance of immune and inflammatory responses in the effects of UE2316. Gene Ontology (GO) analysis was performed using the Database for Annotation, Visualization and Integrated Discovery (DAVID) v6.8. Significance is expressed using the p-value corrected for multiple hypothesis testing using the Benjamini-Hochberg method (q-value). The listed biological processes had  $q < 0.05$ .

<https://doi.org/10.1371/journal.pone.0255709.t001>

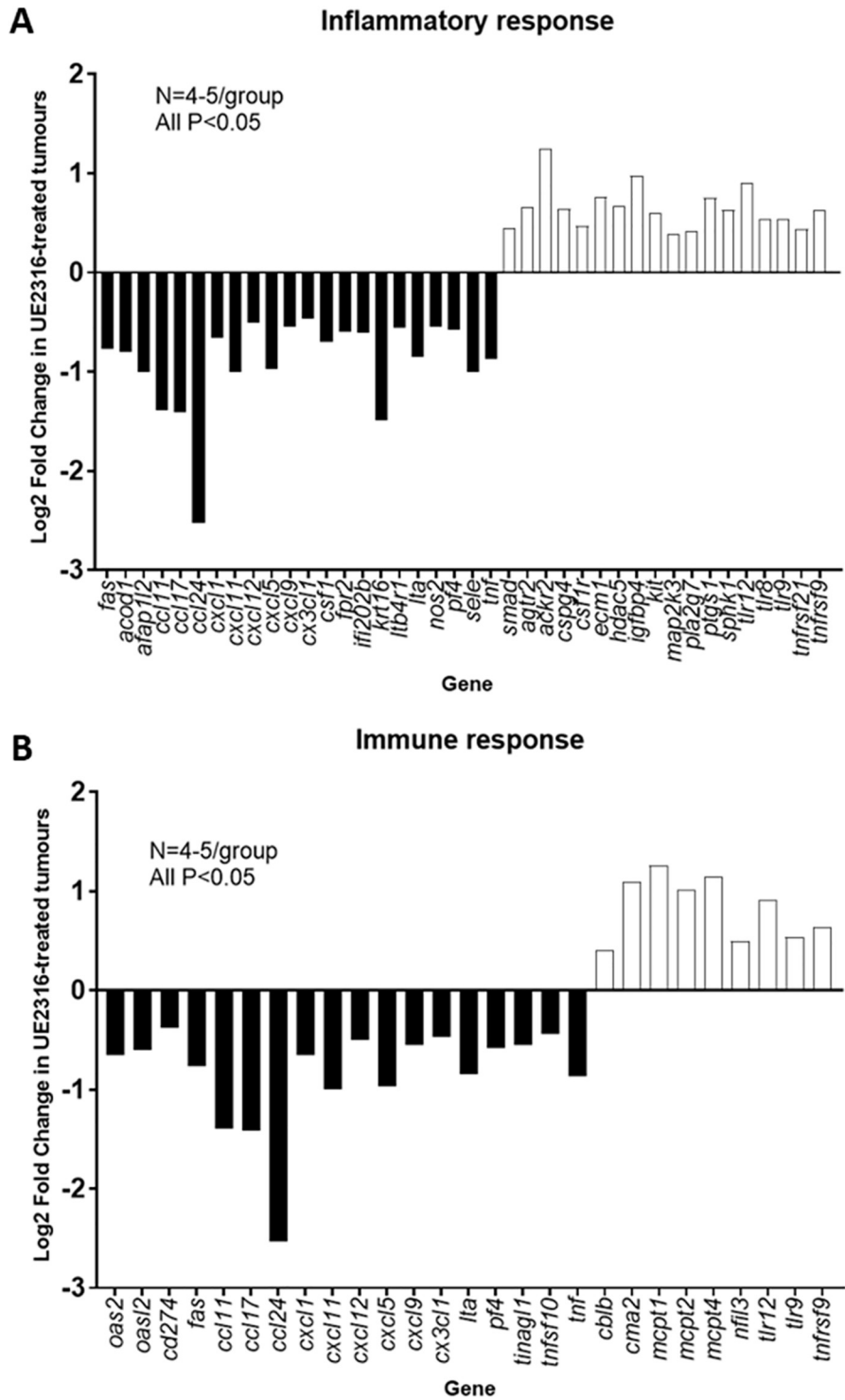


**Fig 7. UE2316 affects inflammatory and immune response genes in SCC tumours; analysed using Gene Ontology analysis.** Differentially-expressed genes identified by RNA-sequencing were defined as being related to the inflammatory response (A) or immune response (B) by Gene Ontology analysis. N = 4-5/group. A modified Fisher Exact test was used to determine whether the proportion of genes in a given list was significantly associated with a biological process compared to the murine genome: P<0.05 for all the above. Data represent mean values with black bars representing genes that are down-regulated in the UE2316-treated tumours and open bars those that are up-regulated.

<https://doi.org/10.1371/journal.pone.0255709.g007>

other studies that report SCC express particularly high levels of GR [28,29], suggesting that SCC may be a more glucocorticoid-sensitive tumour type than PDAC. 11 $\beta$ -HSD1 inhibition did not alter vessel density or *in vitro* tumour cell proliferation, but immune and inflammatory signalling pathways were altered at the transcriptomic level, as was 11 $\beta$ -HSD1 itself. Immune and inflammatory cell content did not differ between control and UE2316-treated SCC tumours, suggesting perhaps that cell behaviour (cytokine environment/activation state) is altered by UE2316. Fluorescence-Associated Cell Sorting of tumours would be required to more elegantly investigate this question in future studies. Generation of Type 1 collagen was reduced at both the transcriptomic and protein level in UE2316-treated SCC tumours; whether this change relates to the altered inflammatory environment remains uncertain.

The only previous study to directly manipulate 11 $\beta$ -HSD1 expression in a solid tumour model demonstrated that 11 $\beta$ -HSD1 overexpression reduced the growth of hepatocellular carcinoma (HCC) tumours in Balb/C nude mice [17], an effect which was apparent over a similar time course as the effect of 11 $\beta$ -HSD1 inhibition shown here (i.e. 3–5 days after cell injection). While the present study supports a role for 11 $\beta$ -HSD1 and local glucocorticoid metabolism in regulating tumour growth from an early stage, a different mechanism may be responsible; the study in HCC identified a significant reduction in tumour angiogenesis, attributed to reduced glycolysis, in tumours overexpressing 11 $\beta$ -HSD1 compared to controls. No evidence of such a process was seen in SCC tumours. The present study made use of a murine tumour cell line able to grow in mice with a functional immune system, a significant strength given that 11 $\beta$ -HSD1 deletion reduces T-cell infiltration in some inflammatory models [30–32] and is likely to influence the tumour microenvironment [33]. Interestingly, both tumour types used in these separate studies (SCC and HCC) were derived from tissues in which 11 $\beta$ -HSD1 is known to play a regulatory role (skin and liver) [34–38].

However, the present study found no evidence of enhanced angiogenesis after 11 $\beta$ -HSD1 inhibition. Enhanced angiogenesis and recovery post-myocardial infarction have been demonstrated consistently in 11 $\beta$ -HSD1 knockout mice [10,11,13,14] and following exposure to the 11 $\beta$ -HSD1 inhibitor UE2316 [39]. The reparative response to myocardial infarction is characterised by increased neutrophil and macrophage recruitment into the myocardium after 11 $\beta$ -HSD1 inhibition [11,14], an effect absent in SCC tumours. Angiogenesis after induced myocardial infarction in rodents is a beneficial process and distinct from the aberrant non-resolving hypoxia-driven angiogenesis seen in tumours [40], which may be mediated by different mechanisms and explain the context-specific effects of 11 $\beta$ -HSD1 inhibition.

Given the lack of evidence that exaggerated angiogenesis promotes SCC tumour growth following 11 $\beta$ -HSD1 inhibition, we considered other mechanisms. The absence of a glucocorticoid-mediated effect on SCC cell proliferation, or any direct effect of UE2316 *in vitro*, strongly suggests that direct proliferative effects on tumour cells are not relevant. However, based on the gene ontology analysis of SCC tumours, the immune and inflammatory responses are likely to be of mechanistic importance. SCC tumours from UE2316-treated mice showed reduced expression of a range of pro-inflammatory cytokine and chemokine genes. These changes were accompanied by an increase in the expression of several members of the *Tlr* and *Tnfrsf* families, and *Csf1r*, suggesting reduced pro-inflammatory ligand binding. Furthermore, expression of a number of interferon- $\gamma$  (IFN- $\gamma$ ) inducible genes was reduced in tumours from UE2316-treated animals. As TLR activation can stimulate the production of IFNs, interleukins and TNF by myeloid and lymphoid cells [18], the evidence points towards reduced inflammatory and immune cell signalling within tumours from UE2316-treated mice. The reduced expression of *Ccl* and *Cxcl* chemokines would predict reduced migration of eosinophils, neutrophils and T-cells into tumours, whilst the reduced expression of 11 $\beta$ -HSD1 itself after UE2316 treatment is indicative of reduced immune/inflammatory cell infiltration and

activation as the enzyme is expressed in macrophages and lymphocytes and upregulated by immune cell activation [3].

The role of inflammation in tumour progression is controversial in that it can both promote tumour progression (including via stimulation of angiogenesis) and inhibit tumour progression (via anti-tumour immunosurveillance). In the present model, 11 $\beta$ -HSD1 inhibition appears to decrease inflammatory signalling whilst enhancing tumour growth, raising the intriguing possibility that UE2316 dampens the anti-tumour immune response. This requires confirmation at the cellular level.

11 $\beta$ -HSD1 inhibition has been shown to influence inflammation previously, but its effects are context-dependent and may vary between acute or chronic inflammation. Similar to induced myocardial infarction, 11 $\beta$ -HSD1 deficiency increases acute inflammation in models of arthritis, peritonitis and pleurisy [41,42]. In obese adipose tissue and atherosclerotic plaques from 11 $\beta$ -HSD1 deficient animals, however, inflammatory and immune cell infiltration is attenuated [30,31]. Arguably, the chronic, non-resolving inflammation and hypoxia seen in obese adipose tissue and atheroma are more similar to the tumour microenvironment than to the ischaemic myocardium; thus mechanistically the latter models may be more relevant.

There is analogous evidence from other models that 11 $\beta$ -HSD1 influences the same inflammatory pathways as we observed here. Wamil *et al.* [30] reported that 11 $\beta$ -HSD1 deletion reduces similar cytokines (including members of the CCL, CXCL and TNF families) in adipose tissue from high-fat diet-fed mice, associated with decreased CD8+ T-cell infiltration and macrophage infiltration in adipose tissue. Michailidou *et al.* [12] found decreased fibrosis in adipose tissue from 11 $\beta$ -HSD1 knockout animals. Furthermore, 11 $\beta$ -HSD1 deletion reduces macrophage and T-cell infiltration into atherosclerotic plaques [32]. Several of the key gene expression changes seen in the present study have also been seen in atherosclerotic plaques after 11 $\beta$ -HSD1 inhibition [31], including reductions in interleukins, toll-like receptors, STAT family members, and several chemokines. The selective 11 $\beta$ -HSD1 inhibitor BVT-2733 was previously shown to improve symptoms of collagen-induced arthritis by reducing the expression of pro-inflammatory cytokines, including TNF, IL-1 $\beta$  and IL6, and reducing inflammatory cell infiltration into joints [43]. Furthermore, the beneficial effects of 11 $\beta$ -HSD1 inhibition in the synovium have been linked to reduced glucocorticoid action in synovial fibroblasts and osteoclasts resulting in a net reduction in damaging inflammation [44].

Although we found effects of 11 $\beta$ -HSD1 inhibition on transcripts in SCC tumours, these were not reflected in demonstrable differences in cell content. Staining for the T cell marker CD3 did not identify a difference between SCC tumours from control and UE2316-treated mice. Likewise, F4/80 staining did not reveal a marked difference in macrophage numbers between treatment groups, yet key transcripts for markers of macrophage polarisation were altered in whole tumour homogenates, suggesting a more subtle effect of 11 $\beta$ -HSD1 inhibition on macrophage content or polarisation.

Cancer-associated fibroblasts and extracellular matrix (ECM) deposition can also influence tumour progression [45–47]. The reduced type 1 collagen seen in SCC tumours mirrors the reduced fibrosis in obese adipose tissue from 11 $\beta$ -HSD1 deficient mice [15], which also showed decreased alpha-smooth muscle actin expression, suggesting reduced fibroblast numbers. Reduced fibrosis and reduced expression of *Col1a1*, *Col1a2*, *Col14a1*, stromal-cell derived factor 1 (*Sdf1*) and *Lox* are all suggestive of reduced fibroblast activity [45,46]. Since fibroblasts can promote anti-tumour immune cell infiltration into tumours [45,47], suppression of fibroblasts by UE2316 could explain the potentially dampened anti-tumour immune response in SCC tumours. Conversely, inflammatory cells are also able to recruit fibroblasts into SCC tumours [48] and this enhanced recruitment can promote SCC growth suppression via the deposition of a fibrotic ECM that constrains tumour cell proliferation and invasiveness.

[49,50], so the effect of UE2316 could be primarily on inflammatory cells or on tumour cells releasing pro-inflammatory signals, with secondary effects on fibroblasts.

Given that only one of the two tumour types examined responded to UE2316 treatment, predicting which tumour types may be more at risk will be important if 11 $\beta$ -HSD1 inhibitors are to be used in at-risk patients. Review of cancer genomics data sets available via the cBioPortal for Cancer Genomics [51] reveals amplification of *HSD11B1* expression in 8–10% of breast and hepatobiliary cancer studies, while around 8% of cutaneous melanomas show either mutation (4%) or amplification (4%) of the gene. Altered expression of *HSD11B1* is also apparent in around 5% of studies on endometrial cancers, non-Hodgkin lymphomas, non-small cell lung cancers and melanomas. Extra vigilance is recommended if 11 $\beta$ -HSD1 use is indicated in patients with such *HSD11B1*-expressing tumours.

In summary, to the best of our knowledge this is the first study to investigate the possibility that pharmacological inhibition of 11 $\beta$ -HSD1 could promote tumour growth by increasing the angiogenic growth of blood vessels. Our results demonstrate that inhibition of 11 $\beta$ -HSD1 in SCC tumours does not alter tumour angiogenesis but dampens immune and inflammatory signalling within the tumour microenvironment, possibly leading to the reduced activation of cancer associated fibroblasts and the reduced deposition of type I collagen. These factors, in combination, may promote SCC growth in this model but relevance to other tumours is uncertain.

## Acknowledgments

The authors are grateful to Marisa Magennis for administrative support.

## Author Contributions

**Conceptualization:** Callam T. Davidson, Morwenna Muir, John C. Dawson, Martin Lee, Stuart Aitken, Scott P. Webster, Natalie Z. M. Homer, Valerie G. Brunton, Patrick W. F. Hadoke, Brian R. Walker.

**Data curation:** Callam T. Davidson, Eileen Miller, John C. Dawson, Martin Lee, Stuart Aitken, Patrick W. F. Hadoke.

**Formal analysis:** Callam T. Davidson, Eileen Miller, Morwenna Muir, John C. Dawson, Martin Lee, Stuart Aitken.

**Funding acquisition:** Valerie G. Brunton, Patrick W. F. Hadoke, Brian R. Walker.

**Investigation:** Callam T. Davidson, Eileen Miller, Morwenna Muir, John C. Dawson, Martin Lee, Stuart Aitken, Natalie Z. M. Homer.

**Methodology:** Callam T. Davidson, Eileen Miller, Morwenna Muir, John C. Dawson, Martin Lee, Stuart Aitken, Alan Serrels, Scott P. Webster, Natalie Z. M. Homer, Ruth Andrew.

**Project administration:** Callam T. Davidson, Ruth Andrew, Valerie G. Brunton, Patrick W. F. Hadoke, Brian R. Walker.

**Resources:** Morwenna Muir, Alan Serrels, Scott P. Webster, Natalie Z. M. Homer, Ruth Andrew, Valerie G. Brunton, Patrick W. F. Hadoke, Brian R. Walker.

**Supervision:** Alan Serrels, Scott P. Webster, Natalie Z. M. Homer, Ruth Andrew, Valerie G. Brunton, Patrick W. F. Hadoke, Brian R. Walker.

**Writing – original draft:** Callam T. Davidson.

**Writing – review & editing:** Callam T. Davidson, Valerie G. Brunton, Patrick W. F. Hadoke, Brian R. Walker.

## References

1. Walker BR. Glucocorticoids and Cardiovascular Disease. *European Journal of Endocrinology*. 2007; 157(5):545–559. <https://doi.org/10.1530/EJE-07-0455> PMID: 17984234
2. Coutinho AE and Chapman KE. The anti-inflammatory and immunosuppressive effects of glucocorticoids, recent developments and mechanistic insights. *Molecular and Cellular Endocrinology*. 2011; 335 (1):2–13. <https://doi.org/10.1016/j.mce.2010.04.005> PMID: 20398732
3. Chapman KE, Holmes M and Seckl J. 11 $\beta$ -hydroxysteroid dehydrogenases: intracellular gate-keepers of tissue glucocorticoid action. *Physiological Reviews*. 2013; 93(3):1139–1206.
4. Seckl JR and Walker BR. Minireview: 11 $\beta$ -Hydroxysteroid Dehydrogenase Type 1—A Tissue-Specific Amplifier of Glucocorticoid Action 1, *Endocrinology*. 2001; 142(4):1371–1376.
5. Zhuang F, Ge Q, Qian J, Wang Z, Dong Y, Chen M et al. Antifibrotic Effect of a Novel Selective 11 $\beta$ -HSD2 Inhibitor (WZ51) in a rat Model of Myocardial Fibrosis. *Frontiers in Pharmacology*. 2021;22; 12:629818.
6. Li H, Sheng J, Wang J, Gao H, Yu J, Ding G et al. Selective Inhibition of 11 $\beta$ -Hydroxysteroid Dehydrogenase Type I Attenuates High-Fat Diet-Induced Hepatic Steatosis in Mice. *Drug Design, Development and Therapy*. 2021; 15:2309–2324.
7. Anderson A and Walker BR. 11 $\beta$ -HSD1 Inhibitors for the Treatment of Type 2 Diabetes and Cardiovascular Disease. *Drugs*. 2013; 73(13):1385–1393.
8. Webster SP, McBride A, Binnie M, Sooy K, Seckl JR, Andrew R et al. Selection and early clinical evaluation of the brain-penetrant 11 $\beta$ -hydroxysteroid dehydrogenase type 1 (11 $\beta$ -HSD1) inhibitor UE2343 (XanamemTM). *British Journal of Pharmacology*. 2017; 174(5):396–408.
9. Folkman J, Langer R, Linhardt R, Haudenschild C and Taylor S. Angiogenesis inhibition and tumor regression caused by heparin or a heparin fragment in the presence of cortisone. *Science*. 1983; 221 (4612):719–725. <https://doi.org/10.1126/science.6192498> PMID: 6192498
10. Small GR, Hadoke PWF, Sharif I, Dover AR, Armour D, Kenyon CJ et al. Preventing local regeneration of glucocorticoids by 11beta-hydroxysteroid dehydrogenase type 1 enhances angiogenesis. *Proceedings of the National Academy of Sciences of the United States of America*. 2005; 102(34):12165–12170. <https://doi.org/10.1073/pnas.0500641102> PMID: 16093320
11. McSweeney SJ, Hadoke PWF, Kozak AM, Small GR, Khaled H, Walker BR et al. Improved heart function follows enhanced inflammatory cell recruitment and angiogenesis in 11 $\beta$ -HSD1-deficient mice post-MI. *Cardiovascular Research*. 2010; 88(1):159–167.
12. Michailidou Z, Turban S, Miller E, Zou XT, Schrader J, Ratcliffe PJ et al. Increased Angiogenesis Protects against Adipose Hypoxia and Fibrosis in Metabolic Disease-resistant 11 $\beta$ -Hydroxysteroid Dehydrogenase Type 1 (HSD1)-deficient Mice. *Journal of Biological Chemistry*. 2012; 287(6):4188–4197.
13. White CI, Jansen MA, McGregor K, Mylonas KJ, Richardson RV, Thomson A et al. Cardiomyocyte and vascular smooth muscle independent 11 $\beta$ -hydroxysteroid dehydrogenase 1 amplifies infarct expansion, hypertrophy and the development of heart failure following myocardial infarction in male mice. *Endocrinology*. 2016; 157(1):346–357.
14. Mylonas KJ, Turner NA, Bageghni SA, Kenyon CJ, White CI, McGregor et al. 11 $\beta$ -HSD1 suppresses cardiac fibroblast CXCL2, CXCL5 and neutrophil recruitment to the heart post MI. *The Journal of Endocrinology*. 2017; 233(3):315–327.
15. Verdegem D, Moens S, Stapor P and Carmeliet P. Endothelial cell metabolism: parallels and divergences with cancer cell metabolism. *Cancer & Metabolism*. 2014; 2;19. <https://doi.org/10.1186/2049-3002-2-19> PMID: 25250177
16. Davidson CT, Dover AR, McVicar CM, Megaw R, Glenn JV, Hadoke PWF et al. Inhibition or deletion of 11 $\beta$ -HSD1 does not increase angiogenesis in ischemic retinopathy. *Diabetes and Metabolism*. 2017; 43(5):480–483.
17. Liu X, Tan X, Xia M, Wu C, Song J, Wu J et al. Loss of 11 $\beta$ HSD1 enhances glycolysis, facilitates intrahepatic metastasis, and indicates poor prognosis in hepatocellular carcinoma. *Oncotarget*. 2016; 7 (2):2038–53.
18. Chapman KE, Coutinho AE, Zhang Z, Kipari T, Savill JS and Seckl JR. Changing glucocorticoid action: 11 $\beta$ -hydroxysteroid dehydrogenase type 1 in acute and chronic inflammation. *The Journal of Steroid Biochemistry and Molecular Biology*. 2013; 137(100):82–92.

19. Azher S, Azami O, Amato C, McCullough M, Celentano A and Cirillo N. The Non-Conventional Effects of Glucocorticoids in Cancer. *Journal of Cellular Physiology*. 2016; 231(11):2368–73. <https://doi.org/10.1002/jcp.25408> PMID: 27115293
20. Serrels A, McLeod K, Canel M, Kinnaird A, Graham K, Frame MC et al. The role of focal adhesion kinase catalytic activity on the proliferation and migration of squamous cell carcinoma cells'. *International Journal of Cancer*. 2012; 131(2):287–297. <https://doi.org/10.1002/ijc.26351> PMID: 21823119
21. McLean GW, Komiya NH, Serrels B, Asano H, Reynolds L, Conti F et al. Specific deletion of focal adhesion kinase suppresses tumor formation and blocks malignant progression. *Genes Dev*. 2004; 18:2998–3003. <https://doi.org/10.1101/gad.316304> PMID: 15601818
22. Hingorani SR, Wang L, Multani AS, Combs C, Deramaudt TB, Hruban RH et al. Trp53R172H and KrasG12D cooperate to promote chromosomal instability and widely metastatic pancreatic ductal adenocarcinoma in mice. *Cancer Cell*. 2005; 7(5):469–83. <https://doi.org/10.1016/j.ccr.2005.04.023> PMID: 15894267
23. Webster SP, Seckl JR, Walker BR, Ward P, Pallin TD, Dyke HJ et al. 4-phenyl-piperidin-1-yl]-[5-(1H-pyrazol-4-yl)-thiophen-3-yl]-methanone Compounds and Their Use. *PCT Intl WO2011/033255*. 2011.
24. Serrels A, Lund T, Serrels B, Byron A, McPherson RC, von Kriegsheim A, et al. Nuclear FAK controls chemokine transcription, Tregs, and evasion of anti-tumor immunity. *Cell*. 2015; 163(1):160–73. <https://doi.org/10.1016/j.cell.2015.09.001> PMID: 26406376
25. Hansen S, Grabau DA, Sørensen FB, Bak M, Vach W and Rose C. The prognostic value of angiogenesis by Chalkley counting in a confirmatory study design on 836 breast cancer patients. *Clinical Cancer Research*. 2000; 6(1):139–146. PMID: 10656442
26. Trapnell C, Pachter L, Salzberg SL. TopHat: discovering splice junctions with RNA-Seq. *Bioinformatics*. 2009; 25(9):1105–1111 <https://doi.org/10.1093/bioinformatics/btp120> PMID: 19289445
27. Trapnell C, Roberts A, Goff L, Pertea G, Kim D, Kelley DR et al. Differential gene and transcript expression analysis of RNA-seq experiments with TopHat and Cufflinks. *Nat Protocols*. 2012; 7(3):562–78. <https://doi.org/10.1038/nprot.2012.016> PMID: 22383036
28. Budunova IV, Carbalaj S, Kang H, Viaje A, Slaga TJ. Altered glucocorticoid receptor expression and function during mouse skin carcinogenesis, *Molecular Carcinogenesis*. 1997; 18(3):177–85. PMID: 9115588
29. Spiegelman VS, Budunova IV, Carbalaj S, Slaga TJ. Resistance of transformed mouse keratinocytes to growth inhibition by glucocorticoids. *Molecular Carcinogenesis*. 1997; 20(1):99–107. PMID: 9328440
30. Wamil M, Battle JH, Turban S, Kipari T, Seguret D, de Sousa Peixoto R, et al. Novel Fat Depot-Specific Mechanisms Underlie Resistance to Visceral Obesity and Inflammation in 11-Hydroxysteroid Dehydrogenase Type 1-Deficient Mice. *Diabetes*. 2011; 60(4):1158–1167.
31. Luo MJ, Thieringer R, Springer MS, Wright SD, Hermanowski-Vosatka A, Plump A et al. 11 $\beta$ -HSD1 inhibition reduces atherosclerosis in mice by altering proinflammatory gene expression in the vasculature. *Physiological Genomics*. 2012; 45:47–57.
32. Kipari T, Hadoke PWF, Iqbal J, Man TY, Miller E, Coutinho AE et al. 11 beta-hydroxysteroid dehydrogenase type 1 deficiency in bone marrow-derived cells reduces atherosclerosis. *The FASEB Journal*. 2013; 27(4):1519–1531.
33. Kim R, Emi M, Tanabe K. Cancer immunoediting from immune surveillance to immune escape, *Immunology*. 2007; 121(1):1–14. <https://doi.org/10.1111/j.1365-2567.2007.02587.x> PMID: 17386080
34. Tiganescu A, Tahrani AA, Morgan SA, Otranto M, Desmoulière A, Abrahams L et al. 11 $\beta$ -Hydroxysteroid dehydrogenase blockade prevents age-induced skin structure and function defects. *Journal of Clinical Investigation*. 2013; 123(7):3051–3060.
35. Terao M, Murota H, Kimura A, Kato A, Ishikawa A, Igawa K et al. 11 $\beta$ -Hydroxysteroid Dehydrogenase-1 Is a Novel Regulator of Skin Homeostasis and a Candidate Target for Promoting Tissue Repair. *PLoS ONE*. 2011; 6(9):e25039.
36. Terao M, Tani M, Itoi S, Yoshimura T, Hamasaki T, Murota H et al. 11 $\beta$ -hydroxysteroid dehydrogenase 1 specific inhibitor increased dermal collagen content and promotes fibroblast proliferation. *PloS ONE*. 2014; 9(3):e93051.
37. Itoi S, Terao M, Murota H, Katayama I. 11 $\beta$ -Hydroxysteroid dehydrogenase 1 contributes to the pro-inflammatory response of keratinocytes. *Biochemical and Biophysical Research Communications*. 2013; 440(2):265–270.
38. Kuo T, McQueen A, Chen TC, Wang JC. Regulation of Glucose Homeostasis by Glucocorticoids. In: Wang JC, Harris C, eds. *Glucocorticoid Signaling. Advances in Experimental Medicine and Biology*, vol 872. New York: Springer; 2015:99–126.
39. McGregor K, Mylonas KJ, White C, Walker BR and Gray G. 216 Immediate Pharmacological Inhibition of Local Glucocorticoid Generation increases Angiogenesis and Improves Cardiac Function after Myocardial Infarction. *Heart*. 2014; 100 Suppl: A118.

40. Chung AS, Ferrara N. Developmental and Pathological Angiogenesis. *Annual Review of Cell and Developmental Biology*. 2011; 27(1):563–584. <https://doi.org/10.1146/annurev-cellbio-092910-154002> PMID: 21756109
41. Coutinho AE, Gray M, Brownstein DG, Salter DM, Sawatzky DA, Clay S et al. 11 $\beta$ -Hydroxysteroid dehydrogenase type 1, but not type 2, deficiency worsens acute inflammation and experimental arthritis in mice. *Endocrinology*. 2012; 153(1):234–40.
42. Coutinho AE, Kipari TMJ, Zhang Z, Esteves CL, Lucas CD, Gilmour JS et al. 11 $\beta$ -Hydroxysteroid Dehydrogenase type 1 is expressed in neutrophils and restrains an inflammatory response in male mice. *Endocrinology*. 2016; 157(7):2928–36.
43. Zhang L, Dong Y, Zou F, Wu M, Fan C & Ding Y. 11 $\beta$ -Hydroxysteroid dehydrogenase 1 inhibition attenuates collagen-induced arthritis. *International Immunopharmacology*. 2013; 17(3):489–94.
44. Hardy RS, Seibel MJ, Cooper MS. Targeting 11 $\beta$ -hydroxysteroid dehydrogenases: a novel approach to manipulating local glucocorticoid levels with implications for rheumatic disease, *Current Opinion in Pharmacology*. 2013; 13(3):440–4.
45. Harper J, Sainson RCA. Regulation of the anti-tumour immune response by cancer-associated fibroblasts. *Seminars in Cancer Biology*. 2014; 25:69–77. <https://doi.org/10.1016/j.semcan.2013.12.005> PMID: 24406209
46. Fang MM, Yuan J, Peng C, Li Y. Collagen as a double-edged sword in tumor progression. *Tumor Biology*. 2014; 35:2871–2882. <https://doi.org/10.1007/s13277-013-1511-7> PMID: 24338768
47. Özdemir BC, Pentcheva-Hoang T, Carstens JL, Zheng X, Wu CC, Simpson TR et al. Depletion of Carcinoma-Associated Fibroblasts and Fibrosis Induces Immunosuppression and Accelerates Pancreas Cancer with Reduced Survival. *Cancer Cell*. 2014; 25(6):719–734. <https://doi.org/10.1016/j.ccr.2014.04.005> PMID: 24856586
48. Coussens LM, Raymond WW, Bergers G, Laig-Webster M, Behrendtzen O, Werb Z et al. Inflammatory mast cells up-regulate angiogenesis during squamous epithelial carcinogenesis. *Genes & Development*. 1999; 13(11):1382–97. <https://doi.org/10.1101/gad.13.11.1382> PMID: 10364156
49. Willhauck MJ, Mirancea N, Vosseler S, Pavesio A, Boukamp P, Mueller MM et al. Reversion of tumor phenotype in surface transplants of skin SCC cells by scaffold-induced stroma modulation. *Carcinogenesis*. 2006; 28(3):595–610. <https://doi.org/10.1093/carcin/bgl188> PMID: 17056607
50. Cretu A, Brooks PC. Impact of the non-cellular tumor microenvironment on metastasis: Potential therapeutic and imaging opportunities. *Journal of Cellular Physiology*. 2007; 213(2):391–402. <https://doi.org/10.1002/jcp.21222> PMID: 17657728
51. Cerami E, Gao J, Dogrusoz U, Gross BE, Sumer SO, Aksoy BA et al. The cBio cancer genomics portal: an open platform for exploring multidimensional cancer genomics data. *Cancer Discovery*, 2012; 2(5):401–404. <https://doi.org/10.1158/2159-8290.CD-12-0095> PMID: 22588877